Interferometric Measurement of Heterogeneous Shear-Layer Spreading Rates

D. W. Bogdanoff*

University of Washington, Seattle, Washington

The spreading rates of the concentration profiles of two-dimensional, low-speed shear layers were measured interferometrically at a velocity ratio of zero and density ratios of 0.2-7. Higher velocities and smaller dimensions were used than in most previous low-speed shear-layer work, so that the Reynolds numbers were similar but the buoyancy effects were much smaller than in earlier investigations. The concentration profiles were found to be self-similar to a high degree and to exhibit a complex transformation of shape, involving both a broadening and a shift toward the low-speed freestream as the density ratio was increased from 0.2 to 7. The present and some earlier experimental results were examined in some detail to assess the effects of buoyancy and the momentum defect at the beginning of the shear layer on shear-layer behavior. It was concluded that some earlier experimental results may have been appreciably affected by buoyancy.

I. Introduction

THE two-dimensional turbulent shear layer has been the subject of much investigation. Birch and Eggers[1] and Birch[2] have compiled surveys of the literature. The three Symposia on Turbulent Shear Flows in 1977, 1979, and 1981 contain many articles on shear layers.[3-5] Unfortunately, there are many inconsistencies and unexplained differences among the various experimental investigations of shear-layer spreading rates. In the present paper, we address only the area of low Mach number shear layers with density ratios (across the shear layer) different from unity. For these shear layers, some of the inconsistencies in previous experimental investigations may be due to buoyancy effects or the the persistent effect of the momentum defect caused by the splitter plate. In the present paper, experimental measurements of the spreading rates of the concentration profiles for shear layers, with velocity ratios λ_u of zero and density ratios λ_ρ of 0.2-7 are presented. ($\lambda_u = u_2/u_1$ and $\lambda_\rho = \rho_2/\rho_1$, where u is the velocity, ρ the density, and subscripts *1* and *2* refer to the high- and low-speed freestreams, respectively.) The measurements were taken with higher velocities and smaller dimensions than those used in most of the previous work, so that the Reynolds numbers were similar to those in earlier investigations, but the buoyancy effects were much smaller.

II. Previous Work

In this section, some earlier experimental investigations are briefly reviewed. We shall frequently refer to the nondimensionalized profiles of velocity and concentration. The nondimensional variables are defined by $u_n = (u - u_1)/(u_2 - u_1)$ and $c = (\rho - \rho_1)/(\rho_2 - \rho_1)$ and vary from 0 in the high-speed freestream to 1 in the low-speed freestream. We shall also make use of the vorticity thickness of the shear layer, defined as $\delta_\omega = \Delta u / [(\partial u/\partial y)_{\max}]$, where y is the dimension normal to the shear layer.

Brown and Roshko[6] have measured velocity and density profiles for shear layers with $\lambda_u = 0.38$, $\lambda_\rho = 0.143$ and 7, and $\lambda_u = 0.143$, $\lambda_\rho = 7$. In these experiments, the flow was directed vertically downward. Fiedler[7] has studied shear layers with $\lambda_u = 0$, $\lambda_\rho = 1$ and 1.09. Here, the flow was directed horizontally and when the flow with $\lambda_\rho \neq 1$ was studied, the lighter gas was on the bottom. Baker and Weinstein[8] have studied shear layers with $\lambda_u = 0.111$, 0.25, and 0.5, $\lambda_\rho = 4$ and $\lambda_u = 0.143$, $\lambda_\rho = 7$. Here, the flow was horizontal, with the heavier gas on the bottom.

Strong arguments can be made that Baker and Weinstein's[8] data are substantially affected by buoyancy. Fiedler's[7] results may have a small (5-10%) buoyancy effect. Buoyancy also may have an appreciable effect on Brown and Roshko's[6] results for $\lambda_u = 0.143$, $\lambda_\rho = 7$. These points will be returned to in Sec. VI, where buoyancy effects in the present and previous experimental results will be discussed in some detail.

There are difficulties with some other investigations of low-speed shear layers with λ_ρ other than unity. Abramovich et al.[9] left a number of important parameters unspecified. The results of Brown and Roshko,[6] Baker and Weinstein,[8] and Abramovich et al.[9] all show that, for λ_ρ significantly different from unity, the nondimensional concentration profile is significantly displaced to the high-density side of the nondimensional velocity profile. The work of Johnson[10] for $\lambda_u = 0.3$ and 0.6, $\lambda_\rho = 4$ is not in agreement in this respect. Rather, for each λ_u value, Johnson's nondimensional profiles of concentration and velocity very nearly coincide. Brown and Roshko's[6] data compilation (their Fig. 10) shows that, for $\lambda_\rho \approx 1$, the variation of δ_ω with λ_u is roughly fitted by $\delta_\omega \propto (1-\lambda_u)/(1+\lambda_u)$, although there is a large amount of scatter. As Brown and Roshko point out several pages later, this relation between δ_ω and λ_u can be easily derived theoretically by a transformation between the spatial and temporal shear-layer problems. Brown's[11] results for $\lambda_u = 0.3$ and 0.6, $\lambda_\rho = 4$ show only a 20% in δ_ω in changing λ_u from 0.6 to 0.3, while the relation $\delta_\omega \propto (1-\lambda_u)/(1+\lambda_u)$ would predict a 115% increase. The relation $\delta_\omega \propto (1-\lambda_u)/(1+\lambda_u)$ is, of course, supported mainly by experimental and theoretical results for $\lambda_\rho = 1$ only. However, Brown[12] gives arguments suggesting that δ_ω varies with λ_u more rapidly than (const) $\times [(1-\lambda_u)/(1+\lambda_u)]$ for $\lambda_\rho > 1$. This would make it difficult to reconcile Brown's[11] results with the trend of the compilation of Brown and Roshko[6] for $\lambda_\rho = 1$.

III. Apparatus

The experimental apparatus is shown in Fig. 1. This apparatus was designed originally for a very different type of experiment which is why there are three parallel nozzles, two

Received Jan. 3, 1983; revision received Feb. 6, 1984.

*Research Engineer, Aerospace and Energetics Research Program. Member AIAA.

shear layers, and a small gap between the nozzle exits and the glass test section walls. (The effects of the test configuration on the quality of the data are discussed in Sec. V.) The nozzle was made of three brass sections with two stainless steel splitter plates. Good seals were obtained by using O-rings and O-ring cord stock with a very large (~50%) squeeze. The contraction ratio of the nozzles was 6. Each nozzle was provided with two orifice plates acting as turbulence screens. The upstream plates had 0.660 mm holes on a 1.067 mm square grid pattern and the downstream plates 0.635 mm holes on a 0.787 mm square grid pattern. The gas flow velocities were determined from manometer pressure readings taken in the three nozzle plenums. The maximum difference between the nozzle plenum pressures and the corresponding pitot tube pressures measured just downstream of nozzle exits was 1.4%. For the taking of the shear-layer data, the three nozzles were run with the same working gas and the nozzle plenum pressures were matched to within 1%. The two shear layers studied originated at the outside edges of the two outside nozzles; the distance between the shear layers was 1.122 cm. The working gases were He, several He/Ar mixtures, CO_2, SF_6 and a SF_6/N_2 mixture. The gases were supplied from cylinders through regulators and metering valves to the nozzle plenums.

Two 50×75 mm optical flats were used to maintain two-dimensional flow in the test section (Fig. 1). These plates were aligned parallel to the nozzle walls using a collimated laser beam and alignment pins set into the bottom of the nozzle block. The spacing and positon of the plates was adjusted to minimize their disturbance of the flow (see Sec. V). On leaving the test section, the jet enters a small diffuser-like channel (catcher), leading to a 15 cm diameter pipe through which the working gases are exhausted by a small air ejector. The catcher and the modest suction of the ejector were necessary to prevent the working gases from boiling up randomly in the optical system light paths outside the test section.

Interferograms were taken parallel to the shear layers using a 5 cm aperture Mach-Zehnder laser interferometer. A 1 mW HeNe laser was used at the light source and the exposures were ~0.1 s, sufficiently long to give good time-averaged data. A lens was used to image the shear layer at the film plane at a magnification of 2.3. Figures 2a and 2b show interferograms for the 84% He/16% Ar and CO_2 jets.

Figure 2c shows a tare (no-flow) interferogram. The simple singlet lens was found to produce significantly distorted images. This was compensated for by placing a square grid at the shear-layer plane, photographing it, constructing a transparent (distorted) grid from this photograph, and reading all the interferograms using the distorted grid. A (distorted) photograph of the grid is shown in Fig. 2d. The interferograms were read manually. Other distortions in the optical system were compensated for by substracting out the fringe shifts of the tare interferograms. For five of the six working gases, fringe shifts were read at four distances from the nozzle exit. For the 62% He/38% Ar working gas, fringe shifts were read at only three distances from the nozzle exit. The distances ranged from 0.35-1.30 cm for the He jet (smallest distances) to 0.49-2.66 cm for the CO_2 jet (largest distances). The distances were limited by system aperture, fringe visibility, and avoidance of the regions where there is interaction between two shear layers or interaction between the shear layer and a wake. The maximum distances from the nozzle exit at which the interferograms were read are denoted by x_{max}. These distances are indicated in Figs. 2a and 2b. It can be misleading to assess the self-similarity of the shear layers from Fig. 2 due to the lens distortion, curvature of the fringes in the tare interferograms, and possible shear-layer interaction for $x > x_{max}$. The self-similarity of the shear layers can be properly assessed from the reduced data (See Sec. IV).

For each working gas, using an optimization scheme, the best origin of the similarity coordinate system ($x_o, y_o = 0$) was

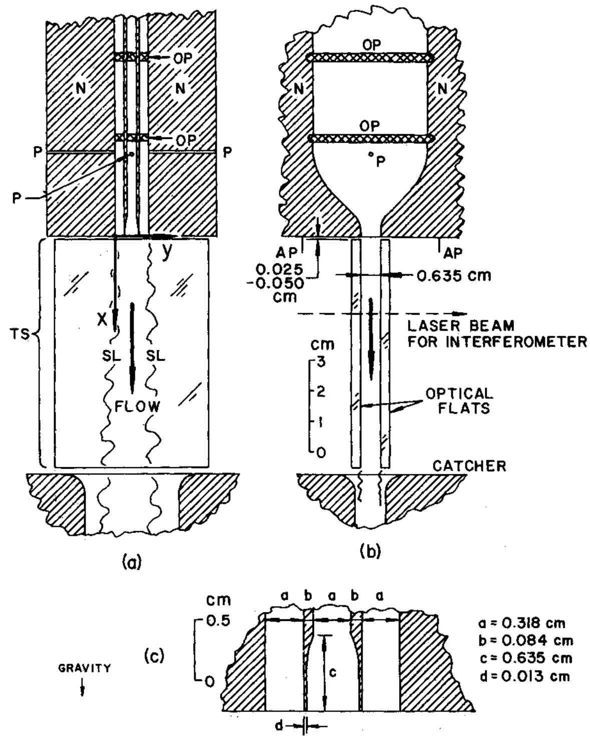

Fig. 1 Experimental apparatus: a) section parallel to shear layers; b) section normal to shear layers; c) 4× magnification of region of a near nozzle exits (N is the nozzle block, P the pressure taps, 0 the orifice plates, TS the test section, and AP the pins used for the alignment of the optical flats and the laser beam; dimensions are in cm).

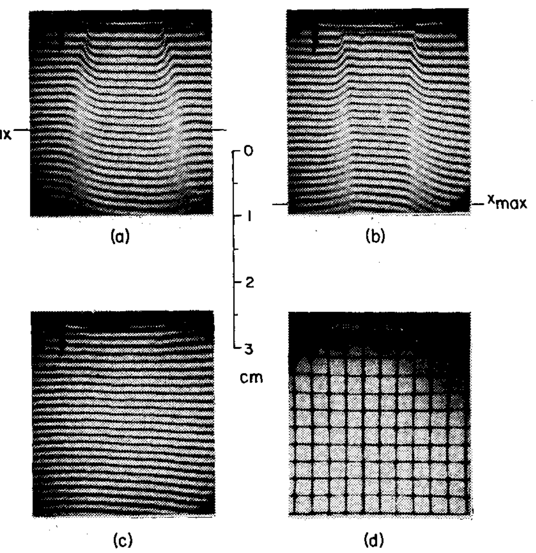

Fig. 2 Interferograms taken parallel to the shear layers: a) 84% He/16% Ar jet, $\lambda_\rho = 2.96$; b) CO_2 jet, $\lambda_\rho = 0.659$; c) tare (no-flow) interferogram; and d) grid used to read the interferograms.

found. (The x,y coordinate system is shown in Fig. 1a at the nozzle exit.) The best value of x_o is defined as that which minimizes a weighted sum of the squares of the differences among the profiles when they are plotted in the form $c = c(\eta) = c[y/(x - x_o)]$. In our optimization scheme, each complete profile was given the same statistical weight, not each data point.

IV. Results

Figure 3 shows the complete sets of concentration data for the CO_2 and 84% He/16% Ar jets. The degree of scatter and self-similarity in Fig. 3 is representative of that of the results for the six working gases. Mean curves for the six working gases were fit by hand to the data. The mean concentration profiles for all six gases are shown in Fig. 4, along with a profile for $\lambda_\rho = 1.09$ taken from Fiedler[7] and discussed in Sec. V. The parameters for the shear layers are given in Table 1. *Re* is the Reynolds number, defined by

$$Re = \bar{\rho}\Delta\mu\delta_{\rho m}/\bar{\mu} \tag{1}$$

where $\bar{\rho} = (\rho_1 + \rho_2)/2$, $\Delta u = u_1 - u_2$, and $\bar{\mu} = (\mu_1 + \mu_2)/2$, where μ_1 and μ_2 are the viscosities of the high-and low-speed freestreams. $\delta_{\rho m}$ is the maximum shear layer thickness calculated by joining the 20 and 80% points of the concentration profiles with a straight line and measuring the distance between the intercepts of this line with the 0 and 100% concentration levels. *Ri* is the Richardson number, defined by

$$Ri = g\Delta\rho\delta_{\rho m}/[\rho(\Delta u)^2] \tag{2}$$

where $\Delta\rho = \rho_1 - \rho_2$ and g is the acceleration of gravity.

The results of Figs. 3 and 4 are presented as observed and are not corrected for the tilt caused by the increase in the displacement thickness (δ^*) of the boundary layers on the glass plates. Since the boundary layers on the glass plates are in the transition region, the increase in δ^* from $x=0$ to $x=x_{max}$ was estimated using Schlicting's formulas for both laminar and turbulent flow (Ref. 13, pp. 141, 638). For each working gas, the larger of the resulting two values of δ^* was used to estimate a corresponding outboard shift of the shear layers, assuming constant pressure in the test section (see Sec. V). The resulting maximum shifts in η are 0.007 for the SF_6, SF_6/N_2, and CO_2 jets, ~0.015 for the He/Ar jets, and ~0.020 for the He jet. If this effect were completely absent, one would expect the profiles to be slightly inboard of where they are shown in Figs. 3 and 4.

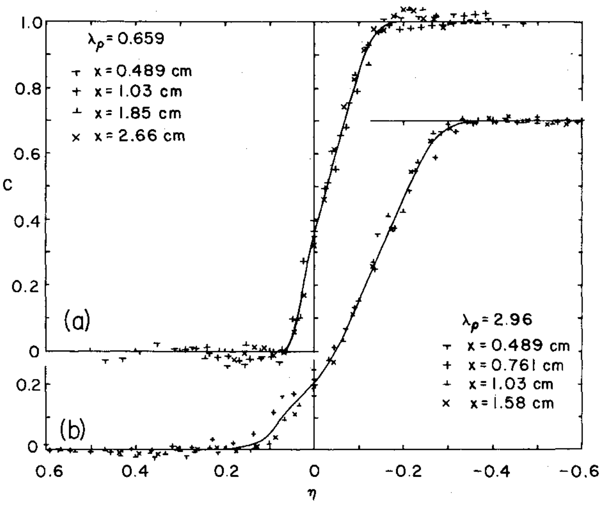

Fig. 3 Complete sets of shear-layer concentration profile data for a) the CO_2 jet, $\lambda_\rho = 0.659$ and b) the 84% He/16% Ar jet, $\lambda_\rho = 2.96$. Ordinate is the concentration of the low-speed stream gas (ambient air) normalized to 0-1; $\eta = y/(x-x_o)$.

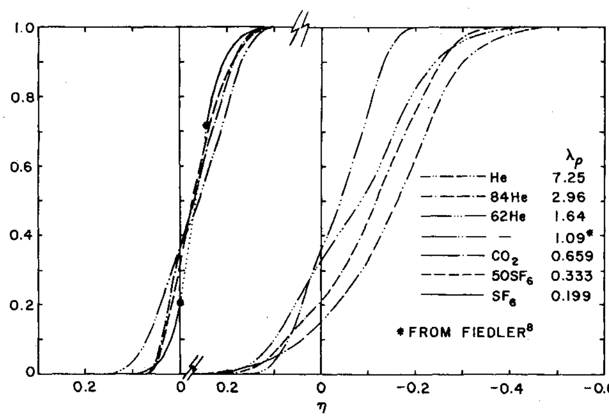

Fig. 4 Mean curves for the shear-layer concentration profiles for the six test gases with λ_ρ of 0.199-7.25. (The coordinate system is the same as in Fig. 3. The identification of the gas mixtures has been abbreviated: 84He means 84%, balance Ar and similarly for the other He/Ar mixtures; $50SF_6$ means 50% SF_6, balance N_2.) Note the break in the η coordinate. The profile for $\lambda_\rho = 1.09$ has been taken from Fiedler[7]; for this profile, Fiedler's values of η have been decreased by 7% (see text).

V. Discussion of Data Quality

Weir and Bradshaw[14] have shown experimentally that for two parallel two-dimensional shear layers with $\lambda_u = 0$, $\lambda_\rho \approx 1$, the interaction between the layers is negligible for $x/h \leq 4$, where h is the distance between the origins of the shear layers. If the thickness of the shear layers are defined using the temperature profiles of Fiedler[8] for $\lambda_u = 0$, $\lambda_\rho \approx 1$, the shear layers are found to meet at $x/h \approx 4.2$. These results imply that, at least for $\lambda_\rho \approx 1$, interaction begins roughly at the point at which the temperature (or concentration) profiles meet. In our studies, data were taken out to only two-thirds of the distance at which the shear layers were estimated to meet; interaction effects should therefore be small.

The thickness of the wakes from the splitter plates (Fig. 1) was determined by operating the center nozzle with one gas and the outer nozzles with a gas of different refractive index. The gas velocities and densities were matched and interferograms were taken parallel to the wakes. Shear-layer data were taken only upstream of the points at which the wakes and shear layers were estimated to meet; wake/shear-layer interaction effects should therefore be small.

Figure 5 shows representative interferograms taken normal to the shear layers. Some distortion of the shear layers is apparent. The effect of these distortions was estimated to produce errors in the concentration profiles (except for the SF_6 profile) of up to ±0.01 for about 95% of the data and up to ±0.015-0.20 in the high-curvature regions of some profiles. For the SF_6 profile, the corresponding numbers are ±0.02 and ±0.025-0.037.

The largest source of error in the concentration profiles is probably human error in the reading of the interferograms. Because of poor fringe visibility, data could be taken for SF_6 only for $c \geq 0.71$ and ≤ 0.21. In Fig. 4, the limiting points for the SF_6 profile (shown by large dots) are joined by a straight line. Since the profiles would be expected to change their shape smoothly as λ_ρ increases, some anomalies are apparent in Fig. 4. (For example, at $c = 0.94$ the profiles for $\lambda_\rho = 1.64$ and 2.96 cross over.) These are very likely artifacts caused by interferogram reading errors.

Pressure measurements were not taken the test section because of the small size of the apparatus and the glass walls of the test section. The maximum measured pressure difference between the interior of the catcher (see Fig. 1) and the ambient air was 0.0013 times the dynamic pressure of the jet q_1. The pressure difference between the interiors of the jets and the ambient air were estimated using a simple mixing length theory, following the method of Tollmein.[15] Tollmein presents a theory for $\lambda_\rho = 1$ only; Golubev[16] describes an extension to $\lambda\rho \neq 1$. Using Tollmein's methods extended to the case $\lambda_\rho \neq 1$, the maximum pressure difference between the jet interior and the ambient air was estimated to be $\sim 0.011 \times q_1$.

In Rebollo's[17] shear-layer experiments with $\lambda_u = 0.38$, $\lambda_\rho = 7$, shear layers with $\alpha = (x/u_1)(du_1/dx) = -0.18$ were found to spread about 50% more rapidly than those with

$\alpha=0$. If we take our maximum estimate of the pressure difference between the jet interior and the ambient air and assume that it changes 50% from $x_{max}/2$ to x_{max}, the corresponding value for α is $\alpha=0.0045$. This is 40 times smaller than the absolute value of α in Rebollo's experiments.[17] From the preceding discussion, it is concluded that pressure gradient effects are very likely small (of the order of 1% or less) in our experimental apparatus.

The shear layers were observed to be self-similar to a high degree. Figure 3 is representative in this respect. For $\lambda_\rho>1$, the virtual origin was downstream of the nozzle exit and x_o was 1-7% of x_{max}(Table 1). For $\lambda_\rho<1$, the virtual origin was upstream of the nozzle exit and x_o was 13-19% of x_{max} (in magnitude)..

Fiedler[7] has obtained temperature profile data for the shear layer between a slightly heated air jet and ambient room temperature still air. Since Fiedler's value of δ_ω for the heated jet ($\lambda_\rho=1.09$), with which the temperature profiles were taken, is about 7% larger than that for the unheated jet ($\lambda_\rho=1.00$), in Fig. 4 we have plotted Fiedler's curve for $\lambda_\rho=1.09$ with the η values reduced by 7%. The agreement between Fiedler's data and the present results is quite good.

VI. General Discussion

Before the present data can be discussed and compared with earlier results, it is necessary to consider the effects of the momentum defect at the beginning of the shear layer and buoyancy in some detail. These phenomena can significantly affect the shear layer.

For a shear layer with $\lambda_u=0$, $\lambda_\rho=1$, Bradshaw[18] has shown that the turbulence intensities $\overline{u'^2}$, $\overline{v'^2}$ and the shear stress $\overline{u'v'}$ do not reach their equilibrium self-similar values until $x/\theta_I\approx 1000$, where θ_I is the momentum thickness of the boundary layer at the beginning of the shear layer. Strong arguments can be made that the criterion $x/\theta_I>1000$ for self-similarity is not appropriate for shear layers where λ_u and λ_ρ differ appreciably from the values in Bradshaw's experiments. For example, for a wake between two identical streams (i.e., a shear layer with $\lambda_u=1$, $\lambda_\rho=1$) shear-layer self-similarity, which requires a disappearance of the wake effects, does not, in general, occur at $x/\theta_I=1000$. Indeed, the wake is usually clearly apparent at substantially greater values of x/θ_I (Ref. 13, p. 742).

It is proposed that an appropriate parameter to assess the importance of momentum defect effects is the ratio R_F of the maximum shear force across the shear layer between the beginning of the shear layer and x [i.e., $x(\overline{\rho u'v'})_{max}$] to the total momentum defect on the splitter plate $(\rho_I u_I^2\theta_I+\rho_2 u_2^2\theta_2)$. We assume that $\bar\rho$ and $\overline{u'v'}$ in $\overline{\rho u'v'}$ can be estimated as $(\rho_I+\rho_2)/2$ and $0.01(u_I-u_2)^2$, respectively. Wygnanski and Fiedler[19] have shown that $(\overline{u'v'})_{max}\approx 0.01(u_I-u_2)^2$ for a shear layer with $\lambda_u=0$, $\lambda_\rho=1$. For simplicity, it is also assumed that $\theta_2=\theta_I$. Using these assumptions, one obtains

$$R_F=0.005\frac{x}{\theta_I}\frac{(1+\lambda_\rho)(1-\lambda_u)^2}{(1-\lambda_\rho\lambda_u^2)} \tag{3}$$

We assume that if R_F is greater than a certain value, the momentum defect effects will be small. Using Bradshaw's x/θ_I criterion for $\lambda_u=0$, $\lambda_\rho=1$ in Eq. (3), the R_F criterion for small momentum defect effects becomes $R_F>10$.

In the preceding discusson, it is assumed that, for cases with $\lambda_u\neq 0$, the thickness of the splitter-plate trailing edge (t_e) is zero and the total momentum defect of the shear layer is due entirely to the momentum defects of the two boundary layers at the beginning of the shear layer. If t_e is appreciable compared to θ_I and θ_2, an additional component must be added in to obtain the total shear-layer momentum defect. A rough estimate for this additional momentum defect is $0.5(\rho_I u_I^2+\rho_2 u_2^2)t_e$.

By visual comparison of the nozzle walls with a steel surface comparator plate, the nozzle wall roughness was estimated to be between 0.8 and 1.6 mm (32 and 64 μin.). The equivalent sand roughness height was assumed to be three times the micrometer roughness value. With this sand roughness height, following procedures outlined in Schlicting (Ref. 13, pp. 213-214, 653-655), θ_I for our shear layers was estimated to be 0.001-0.004 cm. Brown and Roshko's[6] value of θ_I is 0.0025 cm. Fiedler's[7] boundary-layer thickness is given as 0.8 cm. If it assumed that this is the total boundary-layer thickness δ and that $\theta_I=0.097\delta$ (Ref. 13, p. 638), then Fiedler's value of θ_I can be estimated to be 0.078 cm. Using these values of θ_I, the values of R_F at x_{max} were calculated for the experimental results of Brown and Roshko,[6] Fiedler,[7] and the results of the present work.

From Table 2, these values of R_F either exceed the $R_F=10$ criterion or are, at most, 10-15% below this criterion, except for the 62% He/38% Ar jet data ($\lambda_\rho=1.64$) of the present paper. The R_F estimates in Table 2 for Brown and Roshko's[6] experiments do not include the effect of the 0.005 cm thickness of the trailing edge of their splitter plate. This can be estimated, as discussed earlier, to lower their R_F values by a factor of ~2. Konrad[20] performed experiments using the same apparatus as Brown and Roshko and under very similar experimental conditions. From the spreading rate of the wake shown in Konrad's Plate 4d (Ref. 20, p. 110), the total wake momentum defect can be estimated (Ref. 13, pp. 739-743). This momentum defect is a factor of ~5 greater than that calculated using Brown and Roshko's values of θ_I and considering the boundary-layer defects only. Depending, then, on one's estimate for their total splitter-plate momentum defects, Brown and Roshko's values for R_F may be considerably below the values given in Table 2. Particularly, for their $\lambda_\rho=0.143$ case, R_F may be as low as ~2.

In attempting to correlate the self-similarity of the mean density and velocity profiles of Brown and Roshko, Fiedler, and the present work with the corresponding values of R_F, it is important to note that the mean density and velocity profiles may become self-similar long before the detailed turbulence structure does. This is known to be the case for the wake behind a circular cylinder.[21] Bradshaw's[18] criterion and our $R_F=10$ criterion derived therefrom are based on the self-similarity of the detailed turbulence structure.

Richardson numbers (Ri) at x_{max} of the shear layers were calculated, as described in Sec. IV, for the experiments of Baker and Weinstein,[8] Brown and Roshko,[6] Fiedler,[7] and the present work. The absolute value of Ri was calculated to be 0.04-0.25 for Baker and Weinstein's experiments and 0.004-0.006 for Brown and Roshko's experiments, and was 0.0025

Table 1 Shear layer parameters

Gas	u_I,m/s	λ_ρ	$Re\times 10^{-4}$	$Ri\times 10^6$	x_{max}, cm	x_o/x_{max}
He	188.7	7.25	3.47	−2.14	1.30	0.066
84% He/16% Ar	182.8	2.96	4.58	−1.86	1.58	0.008
62% He/38% Ar	89.7	1.64	3.18	−4.53	1.30	0.071
CO_2	80.5	0.659	4.35	3.71	2.66	−0.144
50% SF_6/50% N_2	57.2	0.333	3.09	10.6	1.85	−0.186
SF_6	44.2	0.199	2.50	15.4	1.85	−0.124

for Fiedler's experiments. The absolute value of Ri for the present experiments was $1.8\text{-}16\times10^{-6}$ (Table 1). The value of Ri below which the buoyancy effects should be small can be roughly estimated as follows. Consider a large-amplitude wavy coherent structure pattern in the shear layer. The maximum dynamic pressure developed by the two freestreams passing over the wavy structure will be $P_d \sim 0.5[(\rho_1+\rho_2)/2][(u_1-u_2)/2]^2$. The effective body force developed by this pressure is $F_p \sim P_d/\delta_{\rho m}$. The gravity body force F_g is $\sim g(\rho_1-\rho_2)$. If we assume that buoyancy may be significant if $F_g > 0.1F_p$, the corresponding Richardson number criterion is $Ri > 0.0125$. In Baker and Weinstein's experiments, the flow is horizontal. Their Richardson numbers exceed the criterion given above and the density profiles for three of their four test cases strongly suggest significant buoyancy effects. In Fiedler's data[7] a small buoyancy effect may exist. His flows were also horizontal. The velocity profiles were found to be about 7% wider when the density ratio was 1.09 than when it was 1.00. This difference is in the proper direction for a buoyancy effect.

In Fig. 6, $\delta_{\rho m}/(x-x_o)$ values from Brown and Roshko's, Fiedler's, and the present experiments for $\lambda_\rho \sim 7, \sim 1$, and ~ 0.15 are plotted vs $\phi=(1-\lambda_u)/(1+\lambda_u)$. The data from Brown and Roshko and Fiedler have upper right and upper left tails, respectively. If it is assumed that the central structure of the shear layer moves at a speed u_w, such that the dynamic pressures of the two freestreams with respect to the central structure, i.e., $\rho_1(u_1-u_w)^2/2$ and $\rho_2(u_w-u_2)^2/2$, are equal, u_w can readily be found.[22] If the shear layer is assumed to grow spatially at a rate proportional to $(u_1-u_2)/u_w$ for any given λ_ρ, the variation of $\delta_{\rho m}/(x-x_o)$ with λ_u for a fixed λ_ρ can be calculated. The best fitting curves calculated in this way for the $\lambda_u=0$ and 0.38, $\lambda_\rho \sim 7$ and ~ 0.15 data are shown in Fig. 6 (curves a and b). Since the pairs of λ_ρ values for the two curves are not identical, the curves were calculated for $\lambda_\rho = 7.12$ and 0.169.

Using curves a and b in Fig. 6 for the comparisons, the agreement between the $\lambda_u=0$ and 0.38 values at $\lambda_\rho \sim 7$ and ~ 0.15 is reasonably good. Brown and Roshko's data point at $\lambda_\rho=7$, $\lambda_u=0.143$, however, seems rather high. Buoyancy may be responsible for this high value of $\lambda_{\rho m}/(x-x_o)$. Brown and Roshko's value of Ri for this test case is quite low (3.7×10^{-3}) and, in addition, their flows are oriented vertically downward, which should minimize buoyancy effects. However, their freestream velocity on the low-speed side of the shear layer is very low and consideration of small "balloons" of helium rising on the low-speed side of the shear layer suggests that the "balloon" velocities may be appreciable compared to the low-speed freestream velocity.

The present experimental results should be essentially free of buoyancy effects. In general, the existence of buoyancy effects can be checked for by reversing the orientation of the experiment with respect to gravity.

Referring to Fig. 4, as λ_ρ increases from 0.2 to 7, the concentration profiles change in a complex way, that, on the whole, can be described as a broadening of the profile coupled with a shift of the profile in the outboard (negative η) direction. As λ_ρ increases from 0.199 to 1.09, the profile change is mainly a broadening (i.e., the center of the profile moves only slightly). (The anomalous profile behavior for $c>0.90$ and <0.05 is very likely an artifact caused by interferogram reading errors.) As λ_ρ increases from 1.09 to1.64, the profile continues to broaden, but, in addition, the profile as a whole shifts appreciably outboard. Finally, as λ_ρ increases from 1.64 to 7.25 for $c<0.2$, the main profile change is an outboard shift with little broadening. In this last range of λ_ρ values, broadening continues to be evident for $c<0.2$. A result of the changing modes of profile transformation as λ_ρ increases is that for $c>0.6\text{-}0.7$, the profile moves continuously outboard as λ_ρ increases, but that for $c<0.5$, and particularly for $c<0.25$, the profile first moves inboard as λ_ρ increases from 0.2 but later reverses direction (at $\lambda_\rho=0.6\text{-}1.6$) and moves outboard.

It would be most desirable to obtain more shear-layer data (over a wide range of λ_ρ values) in the small Ri range of the present study, but including velocity profiles and without the hand-interferogram-reading accuracy limitation of the present data.

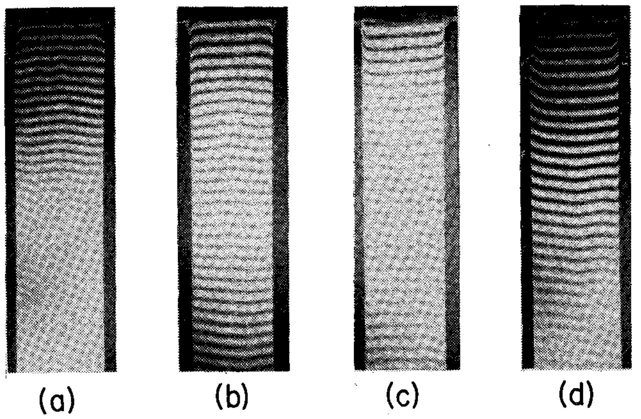

Fig. 5 Interferograms taken normal to the shear layers: a) He, $\lambda_\rho=7.25$; b) 62% He/38% Ar, $\lambda_\rho=1.64$; c) CO_2, $\lambda_\rho=0.659$; d) 50% SF_6/50% N_2, $\lambda_\rho=0.333$.

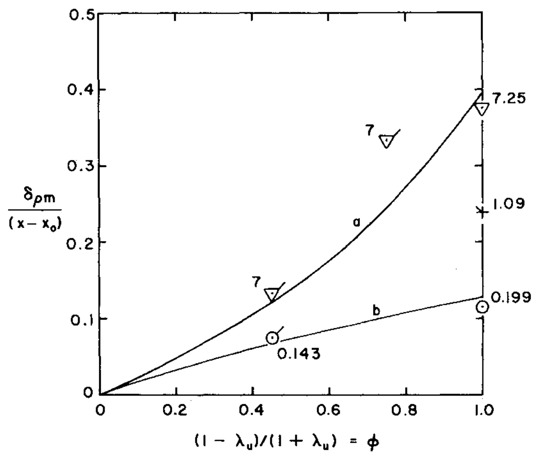

Fig. 6 Shear-layer spreading rates $[\delta_{\rho m}/(x-x_o)]$ plotted vs $\phi=(1-\lambda_u)/(1+\lambda_u)$ with λ_ρ as a parameter. Unflagged data points from present work, points with top right flags from Brown and Roshko[6] and point with top left flag from Fiedler[7]; lines a and b are discussed in the text.

Table 2 Values of R_F

Investigator(s)	λ_u	λ_ρ	R_F
Brown and Roshko[6]	0.143	7	90.3
	0.38	7	30.6
	0.38	0.143	8.71
Fiedler[7]	0	1.09	8.92
Present work	0	7.25	13.7
	0	2.96	11.4
	0	1.64	5.81
	0	0.659	14.0
	0	0.333	9.89
	0	0.199	11.0

VII. Summary

The spreading rates of the concentration profiles of two-dimensional shear layers at a velocity ratio of zero and with density ratios of 0.2-7 were studied. Buoyancy effects in the present work should be negligible. The shear layer spreading rates were determined interferometrically. The shear layers were found to be self-similar to a high degree. The change in the profile shape as the density ratio was increased from 0.2 to 7 was found to be complex, involving both a broadening of the profile and a shift toward the lowspeed freestream. The present results were compared with earlier work and the importance of buoyancy effects and momentum defect (at the beginning of the shear layer) effects in both the present and earlier work was assessed. It was concluded that buoyancy effects may have been significant in some of the earlier experimental measurements.

Acknowledgments

Many conversations with R. E. Breidenthal and W. H. Christiansen were helpful in the course of the work. Much of the difficult designing and machining of the apparatus was done by M. Saynor, D. Peterson, and S. Tillman. The experiments were run with the capable help of R. J. Insuik and S. Tillman. The data reduction and graphics work was capably done by V. Molieri. The research was partially supported by the Air Force Office of Scientific Research, Washington, D.C.

Reference

[1]Birch, S. F. and Eggers, J. M., "A Critical Review of the Experimental Data for Developed Free Turbulent Shear Layers," *Free Turbulent Shear Flows,* Vol. 1, NASA SP-321, 1973, pp. 11-37.

[2]Birch, S. F., "Data Evaluation Report for Free Mixing Layers," Boeing Military Airplane Co., Seattle, Report, Feb. 1980.

[3]*Proceedings of the Symposium on Turbulent Shear Flows,* Pennsylvania State University, University Park, April 18-20, 1977.

[4]*Proceedings of the Second Symposium on Turbulent Shear Flows,* Imperial College, London, July 2-4, 1979.

[5]*Proceedings of the Third Symposium on Turbulent Shear Flows,* University of California, Davis, Sept. 9-14, 1981.

[6]Brown, G. L. and Roshko, A., "On Density Effects and Large Structure in Turbulent Mixing Layers," *Journal of Fluid Mechanics,* Vol. 64, Pt. 4, 1974, pp. 775-816.

[7]Fiedler, H. E., "Transport of Heat Across a Plane Turbulent Mixing Layer," *Advances in Geophysics,* Vol. 18A, Academic Press, New York, 1974, pp. 93-109.

[8]Baker, R. L. and Weinstein, H., "Experimental Investigation of the Mixing of Two Parallel Streams of Dissimilar Fluids," NASA CR-957, 1968.

[9]Abramovich, G. N., Yakovlevsky, O. V., Smirnova, I. P., Secundov, A. N., and Krasheninnikov, S. Yu. "An Investigation of the Turbulent Jets of Different Gases in a General Stream," *Acta Astronautica,* Vol. 14, 1969, pp. 229-240.

[10]Johnson, D.A., "An Investigation of the Turbulent Mixing Between Two Parallel Gas Streams of Different Composition and Density with a Laser Doppler," Ph.D. Thesis, University of Missouri-Columbia, 1971.

[11]Brown, J. L., "Heterogenous Turbulent Mixing Layer Investigations Utilizing a 2-D 2 Color Laser Doppler Anemometer and a Concentration Probe," Ph.D. Thesis, University of Missouri-Columbia, 1978.

[12]Brown, G. L., "The Entrainment and Large Structure in Turbulent Mixing Layers," Paper presented at Fifth Australasian Conference on Hydraulics and Fluid Mechanics, University of Canterbury, Christchurch, New Zealand, Dec. 1974.

[13]Schlicting, H., *Boundary-Layer Theory,* 7th ed., McGraw-Hill Book Co., New York, 1979.

[14]Weir, A. D. and Bradshaw, P., "The Interaction of Two Parallel Free Shear Layers," *Symposium on Turbulent Shear Flows,* Pennsylvania State University, University Park, April 18-20, 1977, pp. 1.9-1.15.

[15]Tollmein, W. "Calculation of Turbulent Expansion Processes," NACA TM 1085, 1945.

[16]Golubev, V.A., "High-Temperature Turbulent Jets," *Turbulent Jets of Air, Plasma and Real Gas,* edited by G.N. Abramovich, Consultants Bureau, New York, 1969, pp. 1-36.

[17]Rebollo, R.M., "Analytical and Experimental Investigation of a Turbulent Mixing-Layer of Different Gases in a Pressure-Gradient," Ph.D. Thesis, California Institute of Technology, Pasadena, 1973.

[18]Bradshaw, P., "The Effect of Initial Conditions on the Development of a Free Shear Layer," *Journal of Fluid Mechanics,* Vol. 26, Pt. 2, 1966, pp. 225-236.

[19]Wygnanski, I. and Fiedler, H. E., "The Two-Dimensional Mixing Region," *Journal of Fluid Mechanics,* Vol. 41, Pt. 2, 1970, pp. 327-361.

[20]Konrad, J. H., "An Experimental Investigation of Mixing in Two-Dimensional Turbulent Shear Flows with Applications to Diffusion-Limited Chemical Reactions," Project Squid Tech. Rept. CIT-8-PU, 1976.

[21]Hinze, J. O., *Turbulence,* 2nd ed., McGraw-Hill Book Co., New York, 1975, p. 505.

[22]Bogdanoff, D.W., "Compressibility Effects in Turbulent Shear Layers," *AIAA Journal,* Vol. 21, 1983, pp. 926-927.